

# Notes

## A $^{15}\text{N}$ CPMAS Study of $N^1, N^2$ -Diaryl-Substituted Polyformamidine, Polyacylamidines, and Polybenzamidines and Model Compounds

Hartmut Komber,\* Christian Klinger, and Frank Böhme

Institut für Polymerforschung Dresden, Hohe Strasse 6, D-01069 Dresden, Germany

Received May 28, 1997

Revised Manuscript Received September 16, 1997

### Introduction

Amidines are of broad interest because of their pharmaceutical, bonding, and ligand properties.<sup>1</sup> We are interested in polyamidines containing the secondary amidine unit  $\text{R}'\text{--N}^1\text{H--CR}=\text{N}^2\text{--R}'$  ( $\text{R} = \text{H}$ , alkyl, aryl) as a polar functional group in the polymer main chain.<sup>2–4</sup>

In such secondary amidines the amino nitrogen acts as proton donor and the imino nitrogen as a proton acceptor. Therefore, low-molecular-weight compounds exhibit prototropic tautomerism in solution. Their solid-state structures are characterized by  $\text{N--H}\cdots\text{N}$  hydrogen bonds (HB) between different molecules. Both the *E*-syn and the *E*-anti configuration have been observed for the amidine structures, depending on residue  $\text{R}$ .<sup>1</sup>

The formation of *cyclic hydrogen-bonded dimers* (Figure 1A) has been proved for formamidines ( $\text{R} = \text{H}$ , *E*-syn configuration). They result in fast prototropic tautomerism in solution.<sup>5</sup> Proton exchange takes place in the solid state as well.<sup>6</sup> Acylamidines ( $\text{R} = \text{alkyl}$ ) and arylamidines ( $\text{R} = \text{aryl}$ ) prefer the *E*-anti configuration of the amidine unit which prevents the formation of cyclic dimers. The proton exchange in solution is much slower for acylamidines and arylamidines than for formamidines. These molecules are bonded by  $\text{N--H}\cdots\text{N}$  hydrogen bonds to *infinite chains* or *linear dimers* in solid state (Figure 1B).<sup>7</sup>

The prototropic tautomerism of  $N^1, N^2$ -diaryl-substituted polyformamidines, polyacetamidines, and polybenzamidines in dimethyl sulfoxide (DMSO) solution has been the subject of a previous study.<sup>8</sup>  $^1\text{H}$ ,  $^{13}\text{C}$ , and  $^{15}\text{N}$  NMR studies proved that the secondary amidine group shows the same characteristics for polymeric compounds as reported on low-molecular-weight compounds.<sup>1</sup> This is valid for both the preferred configuration and for the relative rate of proton exchange on the NMR time scale.

The aim of this paper is to characterize the solid-state structure of these polymers by  $^{15}\text{N}$  cross polarization magic angle spinning (CPMAS) spectroscopy. This method should be particularly useful when studying structural features involving nitrogen atoms.  $^{15}\text{N}$  CPMAS data of polyamidines **1–6** are discussed on the basis of corresponding values obtained from model compounds **7–10**. The prototropic tautomerism of formamidines in the solid state is based on a dynamic  $^{15}\text{N}$

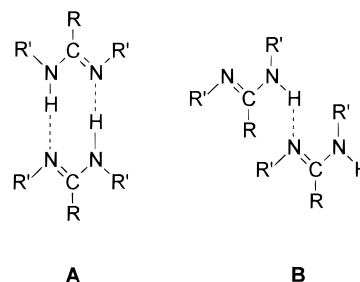


**Figure 1.** Hydrogen bonds between two amidines (A) in *E*-syn configuration forming a cyclic dimer and (B) in *E*-anti configuration forming a linear dimer.

CPMAS study of Männle et al.<sup>6</sup> on  $^{15}\text{N}, ^{15}\text{N}$ -bis(4-bromophenyl)formamidine (**11**).

### Results and Discussion

**Model Compounds.** First insight into the effect of different hydrogen-bonding patterns of secondary acylamidines and arylamidines on their  $^{15}\text{N}$  chemical shifts in the solid state is obtained from model compounds **7–10**. The X-ray structures of **8–10** confirm the *E*-anti configuration of the amidine unit and the absence of cyclic dimers.<sup>9–11</sup> However, different intermolecular  $\text{N--H}\cdots\text{N}$  hydrogen bond patterns have been found. The molecules are joined into parallel chains with a hydrogen-bonded  $\text{N}\cdots\text{N}$  distance of 0.3196 nm for **8**.<sup>9</sup> A more complicated type of chain has been observed for **10**. In this case, the hydrogen-bonded  $\text{N}\cdots\text{N}$  distances alternate between 0.305 and 0.316 nm.<sup>10</sup> A significantly larger value of 0.333 nm can be calculated for the  $\text{N}\cdots\text{N}$  distance between two molecules of the asymmetric unit of *N,N*-diphenylbenzamidines (**9**).<sup>11</sup> Only a single interaction in a dimer of **9** has been reported. From the X-ray data a further  $\text{N--H}\cdots\text{N}$  interaction between the remaining nitrogens and neighboring molecules could be determined. This  $\text{N}\cdots\text{N}$  distance is 0.354 nm.

The great variety of intermolecular and intramolecular geometries of structural similar compounds is reflected in the variation of the  $^{15}\text{N}$  chemical shifts of the imino nitrogen of these compounds (Table 1, Figure 2). For all, except **8**, the amino nitrogen is much less sensitive to structural changes. The lower value for **8** (Figure 2A) may be related to the special type of hydrogen-bonded chains.

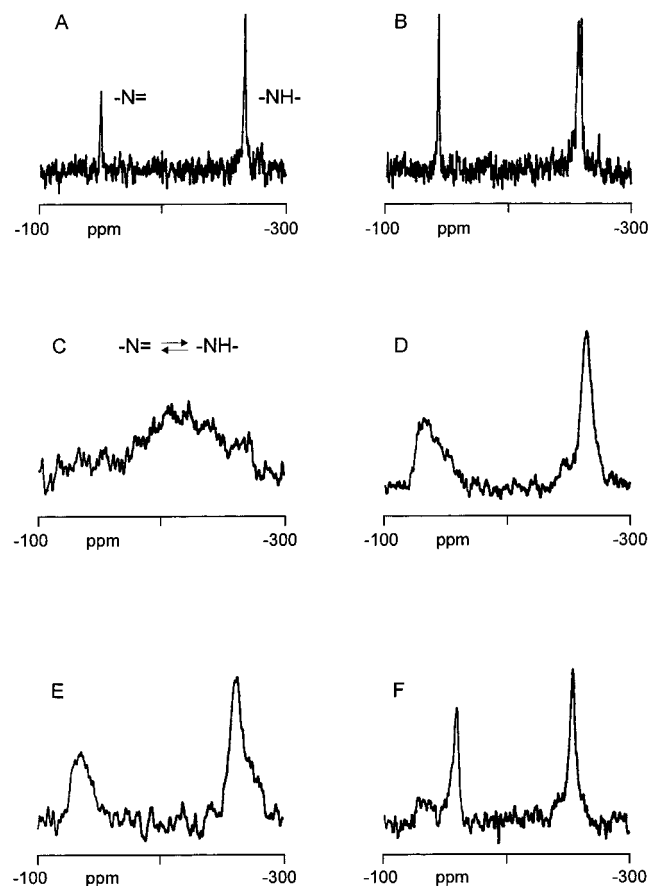
Different substituents  $\text{R}$  and  $\text{R}'$  result only in small  $^{15}\text{N}$  chemical shift effects as can be concluded from the solution data (Table 1). Mainly the interactions in the solid state, particularly the HB patterns, are responsible for the chemical shift changes of the imino nitrogen. Different HB patterns strongly effect  $^{15}\text{N}$  chemical shifts has also been observed for the  $\text{--N=}$  signal of  $\text{NH}$ -pyrazoles in the solid state.<sup>12</sup> Large high-field shifts of the  $\text{--N=}$  nitrogen in the solid state compared to that in solution have been attributed to intramolecular HBs.

Comparing the X-ray data of **9** and **10**, longer  $\text{N}\cdots\text{N}$  distances resulting in a decrease in the strength of the HB interaction are really associated with a more deshielded imino nitrogen. For **10**, the longest  $\text{N}\cdots\text{N}$

**Table 1.**  $^{15}\text{N}$  Chemical Shifts of Polyamidines 1–6 and Model Compounds 7–10 in the Solid State and in DMSO- $d_6$  Solution at Room Temperature

compound	$^{15}\text{N}$ chemical shifts, ppm			
	solid state		DMSO- $d_6$ solution	
	–NH–	=N–	–NH–	=N–
<b>1</b>	–230 <sup>a</sup>		<sup>b</sup>	
<b>2</b> (amorph.)	–264.5	–132 <sup>c</sup>	–264.5	–134.0
<b>2</b> (cryst.)	–254.3	–159.3		
<b>3</b>	–268.8	–136 <sup>c</sup>	–267.4	–136.7
<b>4</b>	–266.1	–136 <sup>c</sup>	–266.5	–135.4
<b>5</b>	–266.7	–133 <sup>c</sup>	–266.4	–135.7
<b>6</b>	–261.7	–134 <sup>c</sup>	–261.8	–135.8
<b>7</b>	–256.7 <sup>d</sup>	–149.5 <sup>d</sup>	–263.3	–132.9
	–258.8 <sup>d</sup>	–151.2 <sup>d</sup>		
<b>8</b>	–266.3	–148.8	–264.5	–134.1
<b>9</b>	–258.1	–137.5 <sup>d</sup>	–261.0	–134.1
		–140.5 <sup>d</sup>		
<b>10</b>	–257.0 <sup>d</sup>	–142.2	–262.1	–136.3
	–259.2 <sup>d</sup>			
<b>11</b> <sup>e</sup>	–257.8	–155.8		

<sup>a</sup> Broad signal. <sup>b</sup> Signal not obtained due to too much exchange broadening. <sup>c</sup> Chemical shift at maximal intensity of a broad signal between –130 and –165 ppm. <sup>d</sup> Two signals may be due to the two molecules in the asymmetric unit. <sup>e</sup> Literature data<sup>6</sup> below the coalescence point of about 115 K; chemical shifts converted to the nitromethane scale: solid  $^{15}\text{NH}_4\text{Cl}$  = –340.8 ppm.

**Figure 2.** Natural abundance  $^{15}\text{N}$  CPMAS spectra of model compounds **8** (A), **10** (B), polyformamidine **1** (C), amorphous polyacetamidine **2** (D), polybenzamidine **6** (E), and crystalline polyacetamidine **2** (F).

distance (0.354 nm) and the most deshielded imino signal (–137.5 ppm) are found. This shift value is in the same range as the DMSO solution data (Table 1). In the solution state the average  $\text{N}\cdots\text{H}-\text{N}$  distance is normally longer than in the solid state.

Two independent molecules in the crystal structures of **9** and **10** may result in a doubling of the amino and

imino signals. This is observed for the imino nitrogen of **9** and for the amino nitrogen of **10** (Figure 2B, Table 1). It is not obvious why only one nitrogen shows this splitting and why this is the imino nitrogen for **9** and the amino nitrogen for **10**. Two signals are observed for each nitrogen of compound **7** with unknown crystal structure (Table 1). From this result two types of HBs with different length are expected for crystalline **7**.

In contrast to formamidines<sup>6</sup> no proton exchange between amino and imino nitrogen could be observed. Measurements at 343 K do not indicate significant signal broadening or chemical shift changes for **7**–**10**. The absence of tautomerism is in accordance with noncyclic HBs between neighboring molecules. A low-field shift of 0.8–1.5 ppm is observed for all imino signals, indicating a weakening of the HBs at elevated temperatures.

**Polymers.** In the  $^{15}\text{N}$  CPMAS spectrum of the polyformamidine **1** (Figure 2C) no separate imino and amino nitrogen signals can be observed. Instead, a broad  $^{15}\text{N}$  NMR signal indicating proton exchange in the solid state is seen. This can be explained by fast proton transfer in cyclic dimers of formamidine groups in *E*-syn configuration (Figure 1A) as reported for solid  $^{15}\text{N}$ ,  $^{15}\text{N}$ -bis(4-bromophenyl)formamidine (**11**).<sup>6</sup> For this compound coalescence of the amino and imino signal has been observed above 115 K. The X-ray structure of  $\text{N}^1, \text{N}^2$ -diphenylformamidine, a model for **1**, confirms such cyclic dimers in the solid state.<sup>13</sup> Obviously, neighboring polymer chains are joined by double hydrogen bonding of formamidine groups. From wide-angle X-ray scattering (WAXS) measurements an X-ray crystallinity of 56% can be determined. This polymer precipitates during melt polymerization and has a low solubility.<sup>4</sup>

In contrast, two  $^{15}\text{N}$  signals are observed for **2**–**6**, similar to what is seen in solution (Table 1). While the NH signal is relatively narrow at –265 ppm, the imino nitrogen appears as a broad, structured signal between –130 and –165 ppm with a maximum at approximately –135 ppm (Figure 2D,E). Both values correspond to the solution data and differ from those of the model compounds with well-defined interactions. Low-field shifted imino signals are also observed for samples of **7** and **9** obtained by quenching a melt in liquid nitrogen. These low-field shifted imino signals indicate that most amidine groups are not involved in a well-defined HB structure. A distribution of  $\text{N}\cdots\text{H}-\text{N}$  distances in hydrogen-bonded associates similar to the solution state better describes the situation. The high-field part of the broad imino signal represents imino nitrogens with stronger hydrogen bonding. A broad distribution of geometries and  $\text{N}\cdots\text{N}$  distances within the solid polymers is in accordance with the amorphous state of melt-polymerized polymers **2**–**6** as confirmed by WAXS measurements.<sup>4</sup>

However, we succeeded in obtaining a more crystalline sample of polymer **2**.<sup>4</sup> A gelation process is observed when a solution of **2** in tetrahydrofuran (5% w/w) is stored at ambient temperature for 3 weeks. A self-organization process resulted in a network of HBs with about 40% X-ray crystallinity after the solvent was evaporated.<sup>4</sup> In the  $^{15}\text{N}$ -CPMAS spectrum of this sample (Figure 2F), both signals are narrowed. The high-field shift of the imino and the low-field shift of the amino nitrogen signal result in chemical shift values which significantly differ from those of the solution state and are similar to the values of the crystalline model

compounds (Table 1). This supports the formation of shorter HBs and is consistent with the high crystallinity determined by WAXS. The residual broad signal at  $-140$  ppm is due to the amorphous component. Although the  $^{15}\text{N}$  chemical shifts of crystalline **2** are similar to those of **11** below the coalescence point<sup>6</sup> (Table 1), the formation of cyclic dimers of acetamidine groups in *E*-syn configuration can be ruled out. Both the amorphous and crystalline sample of **2** were measured at 343 K, and a proton exchange as observed for **1** could not be demonstrated.

## Conclusions

The results presented in this work show that  $^{15}\text{N}$  CPMAS is a useful method to characterize the type and degree of hydrogen bonding in  $N^1, N^2$ -diaryl-substituted polyamidines. The investigated polyformamidine shows fast proton exchange on the NMR time scale due to the formation of cyclic dimers of formamidine groups in mainly crystalline domains. This results in an exchange-broadened  $^{15}\text{N}$  signal.

Both the imino and amino nitrogen signal can be well observed for amorphous polyacylamidines and polybenzamidines. Broad signals and solution-like chemical shifts indicate a broad distribution of  $\text{N}\cdots\text{H}-\text{N}$  distances. The mean value seems to be relatively large and similar to the average hydrogen-bonded  $\text{N}\cdots\text{N}$  distance in DMSO solution. The signals are significantly narrower and shifted to chemical shift values characteristic for crystalline model compounds, if the degree of crystallinity is increased. In this case a more-defined network of HBs is formed. Proton exchange for the solid polyacetamidine could be proved neither for the amorphous nor for the crystalline sample at 343 K.

## Experimental Section

**Materials.** The synthesis of polyamidines **1–6** has been described elsewhere.<sup>4</sup> Acetamidines **7** and **8** were obtained by the reaction of triethyl orthoacetate with aminobenzene and 4-aminotoluene, respectively, using 5 mol % boron trifluoride etherate as a catalyst. Triethyl orthobenzoate, the corresponding amines, and as a catalyst, benzoic acid (5 mol%) were used to synthesize **9** and **10**. All reactions were carried out without solvent at  $140^\circ\text{C}$  bath temperature. The products were recrystallized from ethanol:  $F_p$  (**7**) =  $128\text{--}130^\circ\text{C}$ ,  $F_p$  (**8**) =  $122\text{--}124^\circ\text{C}$ ,  $F_p$  (**9**) =  $148\text{--}151^\circ\text{C}$ , and  $F_p$  (**10**) =  $133\text{--}135^\circ\text{C}$ . The  $^1\text{H}$  and  $^{13}\text{C}$  NMR spectra confirm the structures. Compounds **7** and **9** were prepared with 15% enriched aniline- $^{15}\text{N}$  because the  $^{15}\text{N}$  CPMAS spectra of the unlabeled compounds were of poor quality.

**$^{15}\text{N}$  NMR Spectroscopy.** The NMR measurements were performed on a Bruker AMX-300 spectrometer, operating at 30.41 MHz for  $^{15}\text{N}$ . The sample temperature was maintained at  $\sim 298$  K. The spectra of solutions in  $\text{DMSO}-d_6$  were obtained with inverse gated proton decoupling and referenced to external nitromethane ( $=0$  ppm).

For  $^{15}\text{N}$  CPMAS measurements the samples were spun at 4 kHz in a 5 mm CPMAS probe head from Bruker. Chemical shifts were referenced to external glycine. The solid-state chemical shifts given in this work were converted to the nitromethane scale (glycine =  $-347$  ppm on the nitromethane scale<sup>14</sup>).

Cross polarization experiments were performed with 6.3–7.2 s  $^1\text{H}$   $90^\circ$  pulse duration, a contact time of 5 ms and a recycle delay of 4 s. From 11 000 (**10**) to 40 000 (**1**) scans were accumulated for the  $^{15}\text{N}$  CPMAS spectra of unlabeled samples. The intensity of the imino signal is normally lower than the amino signal intensity (Figure 1).

**Acknowledgment.** The authors gratefully acknowledge the Deutsche Forschungsgemeinschaft for financial support.

## References and Notes

- (1) *The Chemistry of Amidines and Imidates*; Patai, S., Ed.; Wiley & Sons: New York, 1975; Vol. 1; Patai, S., Pappaport, Z., Eds.; Wiley & Sons: New York, 1991; Vol. 2.
- (2) Rillich, M.; Häussler, L.; Jehnichen, D.; Böhme, F. *Polym. Bull.* **1995**, *34*, 43.
- (3) Rillich, M.; Jehnichen, D.; Komber, H.; Böhme, F. *Macromol. Chem. Phys.* **1995**, *196*, 1635.
- (4) Böhme, F.; Klinger, C.; Komber, H.; Häussler, L.; Jehnichen, D. *J. Polym. Sci., Polym. Chem.*, in press.
- (5) Meschede, L.; Gerritzen, D.; Limbach, H.-H. *Ber. Bunsen-Ges. Phys. Chem.* **1988**, *92*, 469.
- (6) Männle, F.; Wawer, I.; Limbach, H.-H. *Chem. Phys. Lett.* **1996**, *256*, 657.
- (7) Kosturkiewicz, Z.; Ciszak, E.; Tykarska, E. *Acta Crystallogr.* **1992**, *B48*, 471.
- (8) Komber, H.; Klinger, C.; Böhme, F. *Polymer* **1997**, *38*, 2603.
- (9) Ciszak, E.; Gdaniec, M.; Jaskolski, M.; Kosturkiewicz, Z. *Acta Crystallogr.* **1988**, *C44*, 2144.
- (10) Alcock, N. W.; Barker, J.; Kilner, M. *Acta Crystallogr.* **1988**, *C44*, 712.
- (11) Alcock, N. W.; Blacker, N. C.; Errington, W.; Wallbridge, M. G. H. *Acta Crystallogr.* **1994**, *C50*, 456.
- (12) Aquilar-Parrilla, F.; Männle, F.; Limbach, H.-H.; Elguero, J.; Jagerovic, N. *Magn. Reson. Chem.* **1994**, *32*, 699.
- (13) Anulewicz, R.; Krygowski, T. M.; Pniewska, B. *J. Crystallogr. Spectrosc. Res.* **1987**, *17*, 661.
- (14) Mathias, L. J.; Powell, D. G.; Autran, J.-P.; Porter, R. S. *Macromolecules* **1990**, *23*, 963.

MA970752M